Cerebral Waveforms for Hemodynamic Assessment

Aarti Sarwal

Qualitative waveform analysis is a key component of interpretation of Transcranial Doppler (TCD) studies in addition to evaluation via quantitative metrics like mean flow velocity (MFV) or pulsatility index (PI) [1]. Normative values for MFVs for intracranial vasculature and PIs are described in literature and mentioned in other chapters of this book [2]. This chapter will focus on qualitative assessment of cerebral hemodynamic waveforms and describe patterns in spectral waveforms that help in assessing cerebrovascular pathology. Many of these characteristic spectral patterns need to be taken in context of the clinical setting, patient presentation, underlying anatomy and pathology being evaluated and should be used as complementary information with disease specific evidence elsewhere in this book.

Vital organs like brain, heart, liver, placenta and kidney all maintain a low resistance circulation to allow preferential blood flow to them in times of shock compared to the rest of the body like the musculoskeletal system and gut where blood vessels feed a high peripheral vascular resistance circulation. Cerebral circulation in addition is unique in its complete dependency on available

A. Sarwal (✉)
Neurology, Neurocritical Care, Wake Forest Baptist Medical Center, Winston Salem, NC, USA
e-mail: asarwal@wakehealth.edu

W. C. Ziai, C. L. Cornwell (eds.), *Neurovascular Sonography*,
https://doi.org/10.1007/978-3-030-96893-9_3

inflow of an oxygenated blood supply to feed the metabolism of neurons and supporting cells with no inbuilt glucose or glycogen sources in the brain. Neurovascular coupling and cerebral autoregulation respond to changes in systemic circulation to preserve cerebral perfusion and ensure blood flow to the brain throughout the cardiac cycle especially diastole. These factors inherently affect the appearance of the spectral waveform on TCD. Transcranial insonation can be performed by imaging Doppler (duplex or B mode guided Doppler) or non-imaging Doppler but for simplicity, all figures will focus on spectral waveforms only when describing pathology, irrespective of accompanying B mode color imaging.

Components of the waveforms Spectral waveforms acquired from pulse wave Doppler imaging of intracranial vessels correspond to the phases of the cardiac cycle with initial 1/3rd of the waveforms representing systole with two components- an up going or acceleration phase and a latter down going deceleration phase (Fig. 1a, b). The following 2/3rd of the waveform represents the diastole or diastolic runoff. The overall waveform has three main characteristics: (1) direction of flow - towards the probe or away from the probe, (2) velocity- time average mean flow velocity, peak systolic velocity and end diastolic velocity and (3) systolic flow acceleration and deceleration slopes (Fig. 1a). A classical intracranial waveform has a sharp early systolic flow acceleration, stepwise late systolic deceleration followed by a robust diastolic run off that maintains 1/4–1/2 of velocities with peak systolic flow throughout the diastole. Systolic phase of systole may manifest three different peaks - P1 (percussion wave triggered by myocardial contractility), P2 (tidal wave created by Windkessel effect or distensibility of arterial wall and subsequent volume displacement), and P3 (dicrotic wave marking the beginning of the diastolic phase and usually follows dicrotic notch (Fig. 1c). These waveforms have been well described in intracranial waveforms visualized on intracranial pressure (ICP) monitors and represent the same hemodynamic phenomena. Pulsations of major arteries and choroid plexus contribute to P1 component. P2

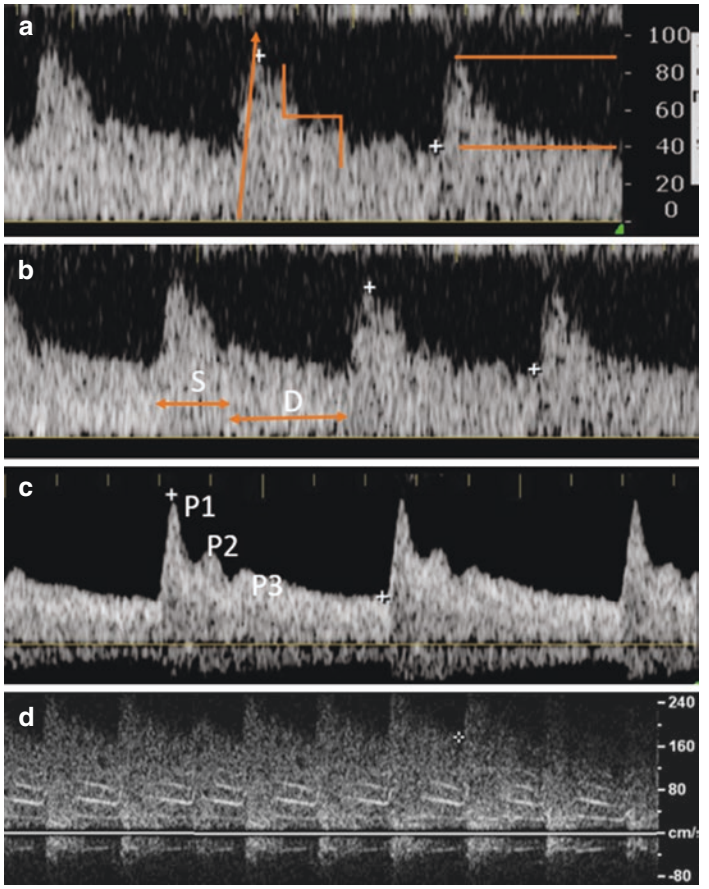

Fig. 1 Normal cerebral circulation represents a low resistance circuit with a rapid upstroke in initial systolic phase followed by a stepwise deceleration (**a**). The initial hump or initial third of the waveform represents the systole (S) and latter 2/3rd represents the diastole (D) in (**b**). The systolic phase has three peaks – P1 representing myocardial contractility, P2 representing arterial distensibility or Windkessel effect and P3 that follows the dicrotic notch hallmarking beginning of diastole (**c**). Figure (**d**) represents an abnormal Doppler spectrum with high mean flow velocity but preserved spectral patterns seen in (**a**–**c**). Bright white lines represent bruits or harmonics that may be created by laminar flow through stenosis

is dependent upon the intracranial compliance and is typically lower than P1 in normal brain. P3 component follows the dicrotic notch of the arterial waveform [3].

On the contrary, the typical wave form of the peripheral circulation or high resistance circulation has a sharp upstroke corresponding to systole but there is reversed flow during early and late diastole giving the classical triphasic oscillating appearance. Such waveforms can be seen in insonation of the external carotid artery or femoral artery [4].

Effect of Cerebral Vascular Resistance on waveforms Many cerebrovascular diseases manifest as changes in resistance of the cerebral vessels or the distal vascular bed (Table 1). Quantitative measures of distal resistance include pulsatility index of Gosling & King - [Peak Systolic Velocity- End Diastolic velocity]/ Mean flow Velocity; and Pourcelot's resistive index - [Peak Systolic Velocity-End Diastolic Velocity]/Peak Systolic Velocity. Resistance changes can have variable effect on the flow and velocity of the blood through the insonated segment dictated by the Spencer and Reid curve (Fig. 2) [5, 6]. This hemodynamic model was classically described for the carotid but is applicable to most vascular lesions in the brain [5]. The correlation of waveforms with the Spencer Reid curve can help understand changes in velocity, flow and resistance and their transitions with progressive lesions.

Qualitatively distal resistance can be assessed by the relationship of the diastolic part of the waveform with the systolic flow. Higher than normal resistance can be seen typically distally in the intracranial circulation during distal vasospasm, hyperventilation, increased

Table 1 Pathological states that affect resistance characteristics of waveforms

Resistance of the cerebral vessels	Resistance of the distal vascular bed
Increased in intracranial stenosis, cerebral vasospasm/ vasoconstriction	Increased in increased intracranial pressure or distal atherosclerotic disease
Decreased in arteriovenous shunting	Decreased in peripheral vasodilatation as in hypercarbia or reperfusion of ischemic brain

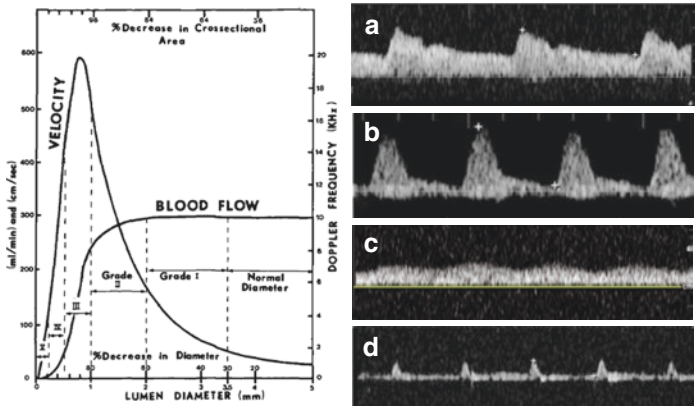

Fig. 2 Spencer and Reid first described a hemodynamic model that explains to a large extent the spectral patterns observed with variations in flow and resistance in progressive stenosis of the carotid artery [5, 6]. This hemodynamic model stands true for most cerebrovascular phenomena observed in transcranial Doppler. (Spencer Reid curve used with permission from Stroke.1979;10:326–330 [6]). (**a**) represents normal cerebral waveforms on right lower corner of the graph with normal diameter, normal flow and normal velocity. (**b**) represents the resistive waveforms expected to be seen in grade II stenosis where velocities are elevated, diastolic flow is compromised and waveforms appear resistive with high pulsatility index. (**c**) represents blunted waveforms in higher grade III stenosis where flow is significantly compromised and velocities are dropping and (**d**) represents near occlusion where minimal flow is seen mostly during systole with significantly low velocities

ICP or as a result of diffuse intracranial atherosclerotic disease (Fig. 3a–3c). Velocity elevation may be the early and only sign of increased vascular resistance in many instances but as luminal stenosis affects flow, different patterns emerge guided by the Spencer Reid curve. Figure 3a, b represents cases where diastolic flow is significantly lower than a 1/4th of systolic, approaches zero or can even be reversed while Fig. 3c represents a relatively normal resistance where elevated MFV is the initial sign of vasospasm. A PI greater than 1.2 in proximal vessels reflects increased distal resistance. Resistance index of 1 denotes no diastolic flow and RI >1 shows reversed EDF and intracranial circulation typically shows RI <1. Distal insonation of the vessels close to the skull may cause physiological changes similar to high resistance especially in the distal MCA and intracranial vertebral insonation that show falsely high PI and RI.

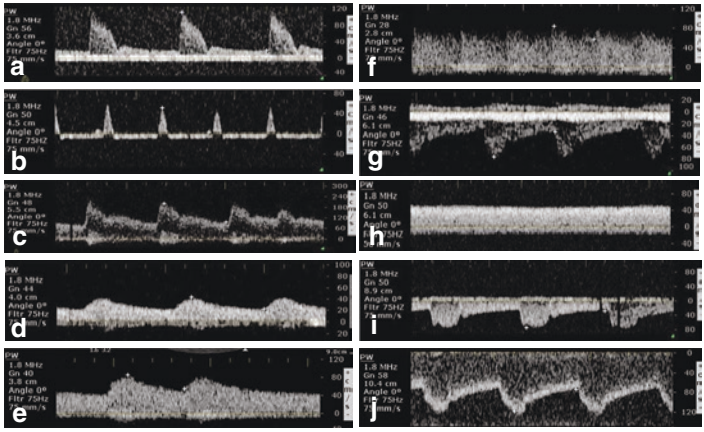

Fig. 3 Resistive waveforms with intact systolic upstroke, downward deceleration can be seen in pre-stenotic segments of focal stenosis or increased intracranial pressure (**a**). Intracranial pressure significantly higher than patient's diastolic pressure can cause reversal of cerebral blood flow during diastole (**b**). Normal cerebral waveforms with physiological relationships of spectral shapes may have elevated velocities, spectral narrowing (white envelope at the upper end of the spectral wave) and bruit (white signal on the baseline at the peak of each systole); such patterns show increased resistance (**c**). Insonation of segments distal to stenosis may show parvus et tardus waveforms (**d**, **e**). Cardiac irregularity can sometimes be noticeable on Doppler studies (**e**) and should be reported. Increased diastolic to systolic ratio can be seen in hyperemic waveforms (**f**). Basilar veins of Rosenthal (white bands with venous waveforms close to the baseline) can often be insonated along with distal posterior cerebral artery (spectral wave below the baseline) (**g**). (**h**) represents the non-pulsatile waveforms seen in patients on coronary bypass. Vertebral and basilar insonation often shows non-compliant waveforms with P2 higher in amplitude than P1 in physiological states (**i**). Spectral narrowing (white envelope at the bottom of the waveform) may be an early sign of increased resistance but has fallen out of diagnostic criteria (**j**)

Lower than normal distal resistance in intracranial vessels manifests in spectral Doppler when flow during diastole exceeds more than 50% of the peak systolic flow. This can be seen diffusely in hypercarbia causing distal vasodilatation-hyperemic waveforms (Fig. 3f). When MFVs are high, analysis of PIs and the spectral waveforms helps distinguish whether vasospasm (high resistance) or hyperemia (low resistance) is causing elevated

velocities. Lindegaard ratios (intracranial middle cerebral artery MFV/ extracranial internal carotid artery MFV) can also help. When lower than normal resistance is seen focally, it usually represents arteriovenous shunting distal to the insonated area (Fig. 3f) or insonation occurring distal to the stenotic lesion (Fig. 3d). Post-stenotic waveforms specifically manifest delayed systolic flow acceleration and deceleration with lower peak velocities classically called *parvus (small) et tardus (late)* (Figs. 3d and 5b) that distinguish them from hyperemic waveforms that may have elevated MFV with normal systolic upstroke but comparatively higher diastolic flow. Severe aortic stenosis could cause all intracranial waveforms to look post-stenotic in the absence of other intracranial lesions. Low resistance waveforms will have a low PI typically <0.6 and very low RI.

Observing qualitative waveform changes in obstructive sleep apnea can be remarkable for low resistance hyperemic waveforms at the end of apneic spells coinciding with hypercarbia which return to normal with initiation of the hyperventilation phase of Cheyne-Stokes breathing. Vasoreactivity test involving inhalation of CO2 or administration of acetazolamide are based on changes in distal vasodilatation caused by hypercarbia driving hyperemic waveforms. Patients with severe anemia or with sickle cell crisis may also demonstrate hyperemic waveforms and looks similar to low resistance waveforms.

Malignant cerebral edema and cerebral circulatory arrest present a unique pattern of increased distal resistance from increased ICPs. Waveforms transition with changes in ICP quite predictably. Resistive waveforms emerge with gradual increase in distal resistance affecting the diastolic component (Fig. 4b). When ICP significantly elevates above patient's diastolic pressure, spectral waveforms may have a reversal of diastolic flow (Fig. 3b). If underlying brain injury progresses and is not amenable to therapy, this waveform classically named oscillating waveforms cannot sustain cerebral perfusion due to lack of diastolic run off necessary for sustaining cerebral oxygenation (Fig. 3b). Anecdotal reports of reversal of this pattern exist when underlying pathology was addressed even if temporarily. Figure 4 represents a hemorrhage with increased ICP patterns on ipsilateral middle cerebral

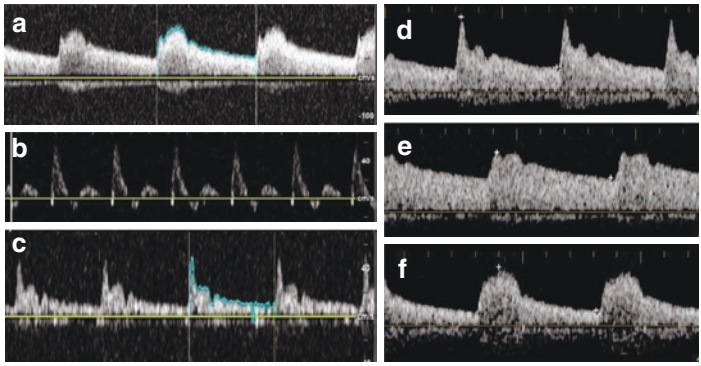

Fig. 4 A young patient with hemorrhagic stroke with insonation of middle cerebral artery ipsilateral to the lesion. Initial waveforms showed a non-compliant waveform with P2 higher in amplitude than P1 (**a**). During an intracranial pressure crisis, the same vessel showed reversal of flow during early and late diastole (**b**). After osmotic therapy administration, the waveforms restored to positive diastolic flow but maintained resistive patterns (**c**). (**d**) represents a normal cerebral waveform in a young compliant brain as a comparison. P2 is same amplitude as P1 in (**e**) whereas it consistently stays higher than P1 in (**f**). Such change in patterns of compliance may be early signs of an impending increased intracranial pressure and need further research

artery insonation (Fig. 4b) that resolved to some extent after hemorrhage evacuation (Fig. 4c) with restoration of forward diastolic flow but ongoing ICP issues. Such cases have elucidated the value of serial TCDs as non-invasive markers of increased ICPs in neurocritical care patients at risk of cerebral edema [7, 8]. Such patterns may be extremely helpful in patients with hepatic encephalopathy who are liver transplant candidates due to challenges in invasive monitoring [9]. Persistence of this pattern despite therapy, however, portends cerebral circulatory arrest [10]. If ICPs continue to rise, oscillating pattern is replaced by systolic hump or spike followed by no flow. Details of cerebral circulatory arrest are described in more detail in another chapter.

Increased resistance localized to a segment of cerebral blood vessels as in intracranial stenosis may produce a sequential transition of spectral waveforms that can help localize the lesion (Fig. 5). Patients may manifest high resistance waveforms when

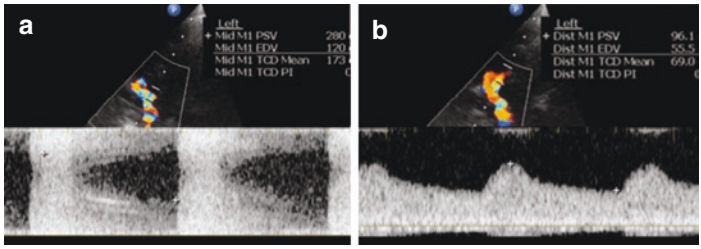

Fig. 5 Patient with subarachnoid hemorrhage complicated by vasospasm had sustained elevation in left middle cerebral artery velocities (**a**) on serial examinations performed daily and was being managed with induced hypertension. During this particular insonation on day 12, no change in mean flow velocity occurred in the left MCA from the previous day (**a**, mean flow velocity 173 cm/s) but the patient had a subtle deterioration in exam. Waveform analysis revealed new finding of a post-stenotic pattern on distal middle cerebral artery insonation (**b**) not seen on prior transcranial Doppler studies suggesting a focal acute MCA flow limiting lesion. Cerebral angiogram revealed a thrombus, and emergent thrombectomy was performed with complete recanalization

insonated proximal to the stenotic segment and low resistance post-stenotic waveforms when insonated distal to the segment with stenosis. Proximal stenotic lesions in the intracranial ICA can cause post-stenotic waveforms in downstream MCA. Due to difficulties in insonation of ICA sometimes this can be the only evidence of hemodynamically significant intracranial ICA stenosis. Figure 5 describes the waveforms in a young patient with subarachnoid hemorrhage on day 12 of her vasospasm watch with high mean flow velocities in the range of moderate-severe vasospasm (173 cm/s, mid segment of middle cerebral artery) but this could be attributable to hyperemia as well, given a favorable relationship between systolic and diastolic flow that points towards low resistance (Fig. 5a). While Lindegaard ratios will be additionally helpful in differentiating these two, the presence of post-stenotic waveforms just distal to the insonated segment directed attention to an acute hemodynamically significant stenosis that incited emergent cerebral angiography (Fig. 5b). Another descriptive example in the follow up of patients being monitored for vasospasm where spectral doppler analysis is helpful, would be progression of waveform patterns to show increased distal

resistance due to increased ICP. Presence of vasospasm with high velocities as seen in Fig. 3c progressing to resistive waveforms in Fig. 3a with apparent normalization of velocities could be a non-invasive marker for diffuse cerebral edema. In both of these cases, assessment of quantitative measures such as velocity alone on serial TCDs would have neglected to bring attention to an acute MCA thrombus discovered on follow up angiogram that was amenable to thrombectomy or diffuse cerebral edema that sequentially decreased diastolic flow in presence of vasospasm without affecting MFV. In these cases, if the neurological exam is limited or confounded, TCD can be a key non-invasive tool to assess patient's cerebral hemodynamics.

Typical flow in a patent vessel is laminar and this may produce clustering of velocities of flowing red blood cells in the vessel lumen. Such clustering is commonly seen in peripheral vessels due to high resistance and called spectral narrowing. In the intracranial circulation, spectral narrowing can be seen in waveforms insonated in stenosed or proximal to high resistance segments (Fig. 3c, j). Extreme cases of spectral narrowing can create harmonics or bruits in the spectral waveforms (Fig. 5a). Spectral broadening is a typical phenomenon seen in turbulent flow downstream of stenosis where laminar flow is interrupted and is a hallmark feature of post-stenotic flow (Fig. 5b). Due to variability of angle of insonation and limitations in adjusting sample size gates to vessel lumen, spectral broadening or narrowing may not be a consistent phenomenon in the intracranial circulation as it is in carotid or peripheral vascular ultrasound and is no longer recommended as a diagnostic criteria. When present, spectral narrowing can be a sign of stenosis (Fig. 3c, j). Another spectral change in stenosed segments could be turbulence- the sonographic correlate of a murmur which can be seen superimposed on the systolic component on the waveform (Fig. 3c).

Effect of cerebral blood flow on cerebral waveforms Flow may be variably affected by resistance. Hence resistive waveforms may progress from preserved to decreased flow as luminal stenosis progresses or vice versa (Fig. 2). Cerebral autoregulation typically targets preserving cerebral blood flow downstream hence presence

of absence of autoregulation may affect changes in spectral waveforms. Patients on systemic vasopressors with intact autoregulation may not manifest any significant change in intracranial waveforms whereas patients with impaired autoregulation may show hyperemic waveforms with induced hypertension or presumed normotension attempted with pressors (Fig. 3f). Such hyperemic injury and its correlate in TCDs is being investigated in post cardiac arrest resuscitation where hyperemic waveforms have been observed during therapeutic temperature modulation and may be a surrogate of reperfusion injury [11]. Another application of ability to distinguish high resistance and high flow states in patients with impaired autoregulation using spectral Doppler is in subarachnoid hemorrhage with vasospasm where induced hypertension continues to be a mainstay. A subset of these patients with impaired autoregulation may continue to have indeterminate velocity elevations with indeterminate ranges in Lindegaard ratios and may be at risk of reperfusion injury after the supposed phase of perfusion dependent delayed cerebral ischemia is over. In post stroke care, emerging reports of flow augmentation across flow limiting lesions not amenable to acute revascularization manifesting as change in spectral patterns on systemic hemodynamic augmentation provide a clinical application and benefit to emergent point of care spectral analysis when existing radiological and clinical information may be insufficient [12].

Collateralization may augment flow in cerebral vessels to compensate for flow limiting lesions. TCD spectral waveforms can be valuable in detecting collateralization patterns [13]. Such collateralization may manifest high velocity waveforms with higher than normal diastolic component or hyperemia waveforms where flow patterns change without obvious change in resistance. Ipsilateral MCA stenosis will often result in hyperemia waveforms in contralateral ACA through AComm recruitment, reversal of ipsilateral ACA and hyperemia in ipsilateral PCA through PComm recruitment eventually leading to reversed ophthalmic recruiting external carotid circulation of the same side. Such patterns of reversal and hyperemia can be a hallmark sign of MCA or intracranial ICA stenosis when either of the vessels cannot be insonated for any reason.

Traumatic brain injury typically shows phasic responses on cerebral blood flow patterns that need more characterization [14]. Limited angiographic studies have shown a hypoperfusion phase followed by hyperemia reperfusion tailed by vasospasm phase in patients with severe TBI [15]. Sonographic characterization of these phases with regard to cerebral blood flow changes and its impact on brain injury needs to be investigated.

Effect of Intracranial compliance effect on cerebral waveforms Lundberg waves and changes in pattern on ICP waves have been long described in the neurocritical care literature [3]. Given the closed compartment created by skull, changes in brain compliance that manifest in ICP waveforms also can be seen in TCD waveforms. The three systolic peaks P1, P2 and P3 can be visualized in spectral waveforms and show similar changes (Fig. 1c). After an ICP crisis, ICP waveforms may have a higher plateau and may manifest decrease in compliance as evidenced by the P2 wave with an equal or greater amplitude than P1 wave (Fig. 4e, f). This results from decrease in the Windkessel effect where decreasing brain compliance decreases the distensability of cerebral blood vessels [9]. This decreased compliance can be seen in TCD waveforms in the anterior circulation in patients who have cerebral edema [9]. It is hypothesized that these patients may have a neurological decline at a lower delta for increased ICP and may need closer monitoring or lower ICP thresholds. Waveforms from insonation of the intracranial vertebrobasilar arteries often show features of decreased compliance in physiological conditions due to the anatomical constraints created by the posterior fossa and do not represent pathology (Fig. 3i). Figure 4 demonstrates a descriptive case with intracranial hemorrhage showing this transition in pattern of P2 relationship with P1 with a compliant waveform (Fig. 4d) on serial assessments on insonation of the middle cerebral artery on the same side as the hemorrhage. Hemorrhage expansion and increase in peri-lesional edema, possibly affected compliance with increase in amplitude of P2 (Fig. 4e, f). Patient suffered an ICP crisis during which the waveforms were noted to be resistive with reversal of flow in early diastole and minimal diastolic flow due to increased distal resistance (Fig. 4b).

Escalating medical therapy and surgical evacuation transitioned the waveforms to positive flow throughout the cardiac cycle though waveforms continue to be relatively high resistance (Fig. 4c). Further investigation needs to be performed in research trials whether addition of spectral Doppler waveform analysis can assist in goal directed therapy in patients at risk of cerebral edema.

Effect of recanalization on cerebral waveforms With wider applications of thrombectomy, recanalization of large vessel occlusions is confirmed by cerebral angiogram and graded by the TICI (Thrombolysis In Cerebral Infarction) score. A similar sonographic grading was proposed to assess recanalization rates after thrombolysis called the Thrombolysis in Brain Ischemia (TIBI) classification [16]. TIBI waveforms are graded as follows: 0, absent; 1, minimal (Fig. 2d); 2, blunted (Fig. 2c); 3, dampened; 4, stenotic (Fig. 2b); and 5, normal (Fig. 2a). In failed recanalization after angiogram, gradual recanalization of thrombosed vessels as evidenced by TCD spectral waveforms can be a correlate of better prognosis. Incidental recurrent thrombosis can be also recognized in high risk patients with confounded exams using spectral waveforms.

Systemic effects on cerebral waveforms Qualitative analysis of the waveforms can be affected in conditions like irregular heart rate (Fig. 3e) or variable pulse pressure. Systemic hemodynamic states such as severe aortic stenosis, presence of heart bypass circuit, can also affect the patterns of spectral waveforms on transcranial Doppler. Patients with severe aortic stenosis may demonstrate post-stenotic waveforms in bilateral anterior and posterior circulation (Fig. 3d). Patient with veno-arterial extracorporeal membrane oxygenation, left ventricular assist devices or undergoing cardiopulmonary bypass intraoperatively for cardiac surgery may have non-pulsatile waveforms (Fig. 3h). In such cases the velocity measured represents the mean flow velocity since the systolic and diastolic phases of the cardiac cycle are missing. Patients with distal atherosclerotic disease especially in advanced age may have higher resistance in distal vessels from non-compliant vessels (Fig. 2b).

Effect of steal of cerebral waveforms Classical description of steal involving vertebral arteries have been extensively studied in relationship to manifest changes in spectral waveforms in neck insonation of vertebral arteries [17]. When steal is severe, changes can also be seen in the intracranial insonation of vertebral arteries through sub-occipital windows. High grades of steal may have complete reversal of vertebral waveforms on affected side with collateralization from opposite vertebral arteries (Fig. 6). Complete reversal of flow in basilar is relatively rare occurrence but has been transiently reported. Rarely, patients with carotid-

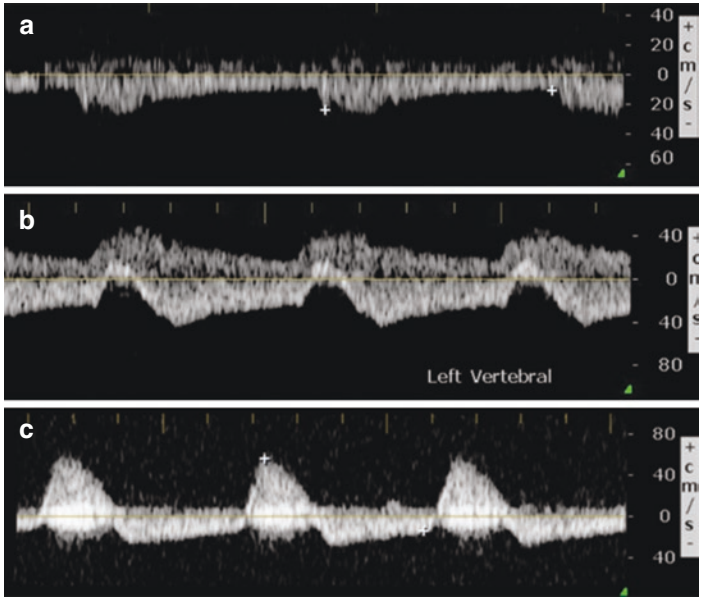

Fig. 6 Vertebral artery waveforms show characteristic waveform changes in presence of subclavian steal syndrome which have been well characterized in literature [17]. Top panel (**a**) shows vertebral vessel insonated via the suboccipital window with flow away from probe showing systolic deceleration. Middle panel (**b**) shows reversal of flow during mid systole that represents a higher grade steal; vertebral artery waveforms are below the baseline with ipsilateral posterior inferior cerebellar artery waveforms superimposed above the baseline. The bottom panel (**c**) shows complete systolic reversal

subclavian bypass procedures with ineffective collateralization across cerebral hemispheres may have intracranial steal waveforms [18]. It is key to note that steal phenomena can be dynamic and triggered by physiological maneuvers like inflating a blood pressure cuff on the same side reducing steal followed by deflation invoking post ischemic reperfusion that may trigger the steal.

Venous compartment of cerebral waveforms Most of the components of the deep cerebral venous system are amenable to insonation by spectral Doppler and show characteristic venous waveforms that appear similar to the blunted waveforms seen in post-stenotic areas on arterial Doppler. The characteristic sound on audible insonation is the *venous hum*. Incidental insonation of basilar veins of Rosenthal is not uncommon during insonation of the distal PCA (Fig. 3g) where a superimposed band of venous spectral Doppler can be seen on the PCA spectrum [18]. The deep middle cerebral veins, basilar vein of Rosenthal, straight sinus, petrosal sinus and transverse sinuses can be insonated via the temporal windows more readily on transcranial duplex with guided B mode. The straight sinus can in addition be insonated via the suboccipital window. More investigations are needed on changes in venous spectral patterns and velocities in different pathologies.

References

1. Alexandrov AV. Extra- and intracranial waveform analysis algorithm, descriptions, classifications, and differential diagnosis. J Vasc Ultrasound. 2015;39(4):192–202.
2. D'Andrea A, Conte M, Scarafile R, Riegler L, Cocchia R, Pezzullo E, et al. Transcranial Doppler ultrasound: physical principles and principal applications in Neurocritical care unit. J Cardiovasc Echogr. 2016;26(2):28–41.
3. Cardoso ER, Rowan JO, Galbraith S. Analysis of the cerebrospinal fluid pulse wave in intracranial pressure. J Neurosurg. 1983;59(5):817–21.
4. Hwang JY. Doppler ultrasonography of the lower extremity arteries: anatomy and scanning guidelines. Ultrasonography. 2017;36(2):111–9.
5. Alexandrov AV. The Spencer's curve: clinical implications of a classic hemodynamic model. J Neuroimaging. 2007;17(1):6–10.

6. Spencer MP, Reid JM. Quantitation of carotid stenosis with continuous-wave (C-W) Doppler ultrasound. Stroke. 1979;10(3):326–30.
7. Cardona P, Quesada H, Cano L, Campelacreu J, Escrig A, Mora P, et al. Oscillating transcranial Doppler patterns of brain death associated with therapeutic maneuvers. Pers Med. 2012;1(1):321–4.
8. Kumar G, Alexandrov AV. Vasospasm surveillance with transcranial Doppler sonography in subarachnoid hemorrhage. J Ultrasound Med. 2015;34(8):1345–50.
9. Aggarwal S, Brooks DM, Kang Y, Linden PK, Patzer JF II. Noninvasive monitoring of cerebral perfusion pressure in patients with acute liver failure using transcranial doppler ultrasonography. Liver Transpl. 2008;14(7):1048–57.
10. Ducrocq X, Hassler W, Moritake K, Newell DW, von Reutern GM, Shiogai T, et al. Consensus opinion on diagnosis of cerebral circulatory arrest using Doppler-sonography: Task Force Group on cerebral death of the Neurosonology Research Group of the World Federation of neurology. J Neurol Sci. 1998;159(2):145–50.
11. Iordanova B, Li L, Clark RSB, Manole MD. Alterations in cerebral blood flow after resuscitation from cardiac arrest. Front Pediatr. 2017;5:174.
12. Gomez J, Wolfe S, Sarwal A. Sonographic demonstration of a perfusion-dependent stroke with negative MRI and a flow-limiting stenosis. Neurocrit Care. 2020;32(3):883–8.
13. Muller M, Hermes M, Bruckmann H, Schimrigk K. Transcranial Doppler ultrasound in the evaluation of collateral blood flow in patients with internal carotid artery occlusion: correlation with cerebral angiography. Am J Neuroradiol. 1995;16(1):195–202.
14. Ziegler D, Cravens G, Poche G, Gandhi R, Tellez M. Use of transcranial Doppler in patients with severe traumatic brain injuries. J Neurotrauma. 2017;34(1):121–7.
15. Inoue Y, Shiozaki T, Tasaki O, Hayakata T, Ikegawa H, Yoshiya K, et al. Changes in cerebral blood flow from the acute to the chronic phase of severe head injury. J Neurotrauma. 2005;22(12):1411–8.
16. Demchuk AM, Burgin WS, Christou I, Felberg RA, Barber PA, Hill MD, et al. Thrombolysis in brain ischemia (TIBI) transcranial Doppler flow grades predict clinical severity, early recovery, and mortality in patients treated with intravenous tissue plasminogen activator. Stroke. 2001;32(1):89–93.
17. Kliewer MA, Hertzberg BS, Kim DH, Bowie JD, Courneya DL, Carroll BA. Vertebral artery Doppler waveform changes indicating subclavian steal physiology. Am J Roentgenol. 2000;174(3):815–9.
18. Baumgartner RW, Gönner F, Arnold M, Müri RM. Transtemporal power- and frequency-based color-coded duplex sonography of cerebral veins and sinuses. AJNR Am J Neuroradiol. 1997;18(9):1771–81.